HIGH POWER FELS DRIVEN BY RF SUPERCONDUCTING LINACS

George R. Neil
Thomas Jefferson National Accelerator Facility (Jefferson Lab), 12000 Jefferson Avenue,
Mail Stop 6A, Newport News, VA 23606, USA

Abstract

High power Free Electron Lasers (FELs) have been an elusive promise since the development of FEL oscillators over two decades ago. Limitations in duty factor, ability to carry high brightness beam, and the high cost of RF wall losses has stymied progress in room temperature accelerator systems. The application of SRF technology has now permitted two orders of magnitude increase in FEL average power and at the same time shown that high quality FEL beam can be produced by the first demonstration of lasing at the 5th harmonic of the fundamental. A concurrent key technical development which leverages the high efficiency of SRF linacs was the demonstration of beam energy recovery while lasing. This leads to high overall efficiency, especially in high average power systems. This paper will discuss the issues relating to SRF use in high average power FELs and present the results of the IR Demo FEL at Jefferson Lab demonstrating the sizeable advantages that SRF offers for kilowatt average power output.

1 INTRODUCTION

Free Electron Lasers place large demands on the builders of the driver accelerators. The energy must be high to deliver short wavelengths as set by the basic FEL resonance equation.

$$\lambda_s = (\lambda_w/2\gamma^2)(1+K^2) \qquad (1)$$

where λ_s is the output wavelength, λ_w the wiggler wavelength, γ the relativistic factor, and K is the wiggler strength parameter. $K = 0.934\, B_{rms}(T)\, \lambda_w(cm)$ with B_{rms} the wiggler field.

The FEL requires high peak currents in order to achieve sufficient gain to lase. This charge must be delivered with minimal degradation of the transverse and longitudinal emittances if the high gain is to be preserved. This design challenge becomes especially acute at short wavelengths. The small signal gain of the FEL is given by[1]

$$G = 29.4\, (I/I_A)(N_w^2/\gamma)B\eta_l\eta_f\eta_\mu \qquad (2)$$

where I is the current, I_A is the Alfven current = 17 kA, N_w is the number of wiggler periods, $B = 4\xi[J_0(\xi)-J_1(\xi)]^2$ where $\xi = K^2/[2(1+K^2)]$. The last three terms (η_l, η_f, η_μ) account for emittance and energy spread effects, gain degradation due to imperfect beam overlap, and slippage between the electrons and the optical pulse.

For optimum coupling to occur the optical beam must overlap the electron beam through the wiggler. In addition, due to finite emittance the betatron motion of electrons in the wiggler causes them to sample variations in the wiggler field leading to an effective energy spread. This sets a soft limit on the emittance ε of the electron beam for achieving a particular wavelength given by

$$\varepsilon < \lambda/4\pi\,, \quad (\lambda/4\pi)(\beta/L_{1D}) \qquad (3)$$

for oscillators [1], and amplfiers [2].

Likewise the gain of the FEL falls off if the energy spread is too large in both oscillators and amplifiers because the electrons to fall out of resonance with the pondermotive wave.

$$dE/E < 1/(4\pi N_w)\,, \ (1/4\pi)(L_{1D}/\lambda_w) \qquad (4)$$

Here β is the matched envelope function of the wiggler and L_{1D} is the 1 dimensional gain length. These criteria, though soft, allow for the choice of FEL accelerator performance from essentially first principles. Figure 1 and 2 illustrates how fast gain length and power degrades for

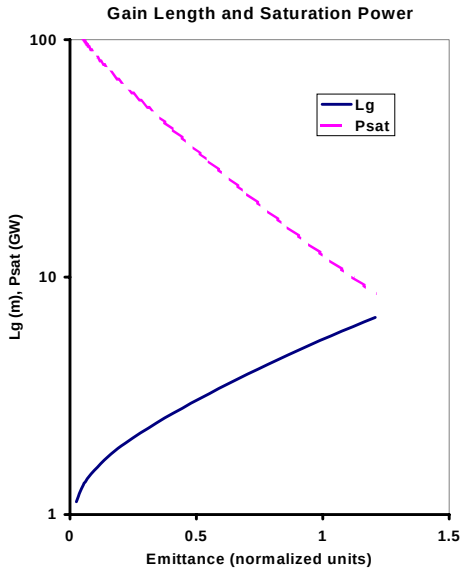

Figure 1: Decrease of gain length and saturation power as the emittance is varied. The normalization factor is given in equation (3).

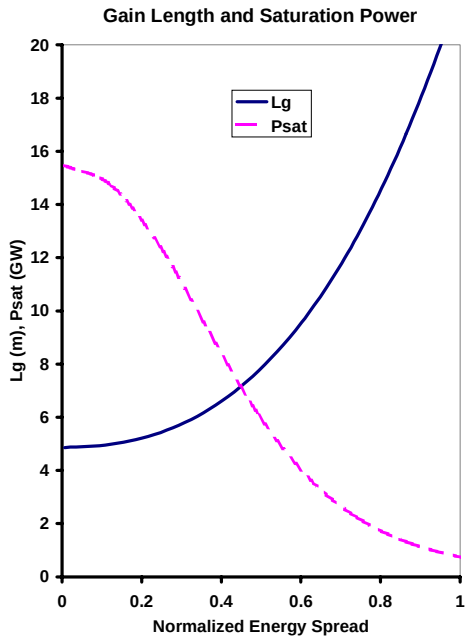

Figure 2: Decrease of gain length and saturation power as a function of the normalized energy spread of equation (4). The calculation is for the same parameters as Figure 1. The emittance is 1.5 mm mrad normalized. An energy spread of 1.0 corresponds to 0.106% dE/E.

one set of parameters. It is clear that degradations of factors of 2 in emittance or energy spread are generally intolerable for FEL accelerators when operating near their short wavelength limits. The calculation is for parameters considered for the SLAC LCLS 4th Generation Light source and is based on formulas in [2]. The beam energy is 15 GeV, the peak current is 5 kA, , the wiggler wavelength is 3 cm, and the wiggler K is 3.7. The energy spread is 0.02%. An emittance of 1.0 corresponds to approximately 1.5 mm mrad normalized.

Additional performance goals are often set by the FEL linac designer. For a useful device the designer wants exceptional wavelength stability which translates directly into linac energy stability (the wavelength moves 2% for every 1% energy shift). There are also phase stability requirements of the beam at the wiggler which sets stability limits on the master oscillator system, the rf phase control, and through dispersive path length coupling, the beam energy stability. Treatment of these is beyond the scope of this article except to say that CW operation of the linac generally offers advantages in phase and amplitude control for stability. We refer the reader to [3].

The designer of such a linac system often wants these qualities at high duty factor, either to achieve high average power or to supply light to many different users through a switching system. Superconducting rf technology is uniquely suited to provide an answer to these requirements and provide additional benefits besides. We discuss these design drivers in depth below, provide some scaling arguments, and then illustrate their implication by example of their application to one system already operational and one planned.

2 DESIGN CHOICES

In choosing a linac technology – copper or srf – for an FEL linac there are both physics issues and system level design factors which lead one to the srf approach when high power or high duty factor is desirable. In this regard the design drivers for high power FELs are similar to those of other high current systems such as B factories and reviews such as [4] offer excellent guidance in design choices. The physics issues to consider include beam breakup (BBU) instabilities, wakefield generation, and beam energy and phase stability. The system level design drivers include the ability to operate CW for high duty factor and/or high average power, the ability to incorporate energy recovery for several key benefits including reduced capital investment, and higher operating efficiency for reduced operating costs. We will treat the physics issues first.

2.1 Physics Issues

Every relativistic beam transport system causes some degradation to the electron beam quality. It is important to ensure that this degradation does not lead to a significant reduction in performance of the FEL. As was shown above there are fairly sharp cliffs beyond which good performance of the FEL is exceedingly hard to obtain.

One effect which causes an increase in energy spread of the micropulses is longitudinal wakefields which occur any time a relativistic beam passes through an aperture or change in pipe diameter. The effect scales like

$$dE \sim Q N_{cavities} (g N_{cell}/\sigma)^{1/2}/a \qquad (5)$$

where $N_{cavities}$ is the number of accelerator cavities in the linac, N_{cell} is the number of cells per cavity, g is the gap, a the aperture, and σ is the micropulse length of the charge Q [5].

While the micropulse length has no particular dependence on whether the design is copper or srf, the other terms do depend on this. To reach a particular energy requires a certain number of cavities operating a particular gradient. We have chosen a specific copper cavity design and a srf cavity design from [4] to illustrate the frequency dependencies. For this comparison the HOM loading of a copper cavity was 0.34 V/pC while an identical frequency srf cavity was 0.11 V/pC. Since the shunt impedance is not such a design driver for srf cavities much larger apertures are generally used. The fundamental R/Q was 265 Ohm/cell for the copper cavity and 89 Ohm/cell for the SRF cavity. It is assumed that the cavity geometry scales with frequency although physically it is easier to damp HOMs in larger structures.

The maximum gradient achievable scales with frequency and whether the system is pulsed or CW. For copper systems operating CW the gradient limit is set by the cooling capability so the heat flux was held constant as frequency was varied. This results in gradient scaling as $(\text{frequency})^{-1/4}$. In pulsed operation the gradient limit is field emission which has an entirely different dependence. The operational limits are generally chosen as some factor times the Kilpatrick limit [6], E_{kp} given by (in transcendental form with E_{Kp} in MV/m and f in MHz)

$$f = 1.64\, E_{Kp}^{\ 2}\, e^{-(8.5/E_{kp})} \qquad (6)$$

This typically drives CW copper machines to low frequency and pulsed machines to as high a frequency as the beam will remain stable at. A known operating value of 3 MV/m at 405 MHz for CW and 50 MV/m pulsed at 2700 MHz set the absolute scales.

For the SRF cavities different factors come in to play and in the past the scaling limits for an ensemble of cavities have been dominated by surface imperfections when operating CW [7]. These scale as the cavity surface area or $(\text{frequency})^{-2}$. Significant differences are often found between single cell cavities at a particular frequency and multi-cell cavities. Reductions in operating gradient are also invoked between test stand data and beam operations. As cleaning techniques and the quality of niobium has improved these scaling limits have become less clear. There are many examples now of high gradient cavities at low frequencies which exceed previously believed limits by substantial margins (Fig. 3). There should still be improvement as one goes to higher frequencies and so we have conservatively chosen a linear scaling with frequency to illustrate the beam scaling factors. As more data becomes available and the true limits appear these curves should be updated appropriately.

The difference in limits between pulsed and CW are not as clearly established as in the case of copper machines but factors of two differences between CW and pulsed operation have been seen. It seems likely that srf cavities are subject to Kilpatrick limits just as copper machines are although the care with which srf cavities are generally treated and the excellent vacuum environment suggests that different safety factors may be applied. There is only a small amount of experiential data available so a value of 1/2 the pulsed gradient limit of copper cavities at the same frequency was used. One example is the TTF design value of 24 MV/m for their 9-cell 1300 MHz cavity. A pulsed copper cavity at this frequency would operate at 55 MV/m. This choice should also be revisited as further data becomes available. Care should be used in applying these results since there are many cavity operating condition dependent parameters that could materially affect the results. Nonetheless it is a useful starting point for system trades. Figure 3 shows the gradient limits assumed in the stability illustrations which follow.

Figure 4 shows the frequency scaling for copper and srf machines operating pulsed or CW. It is clear from the curves that no particular advantage for srf exists if operating at low duty factor due to the high gradients that copper machines can achieve. Operating CW brings a sizeable competitive advantage to srf linacs in terms of minimizing beam degradation by longitudinal effects.

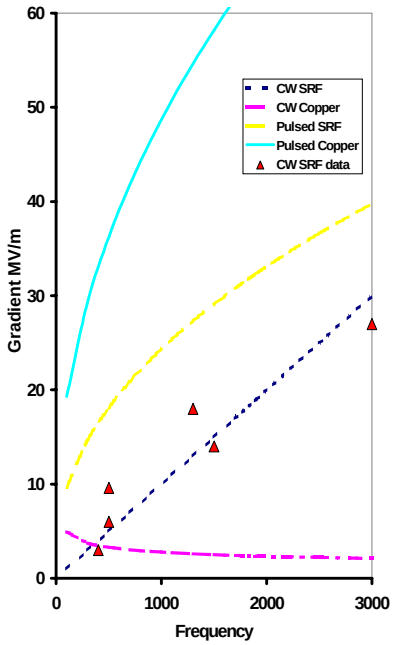

Figure 3: Gradient limits for pulsed and CW copper and srf linacs assumed in the stability calculations below.

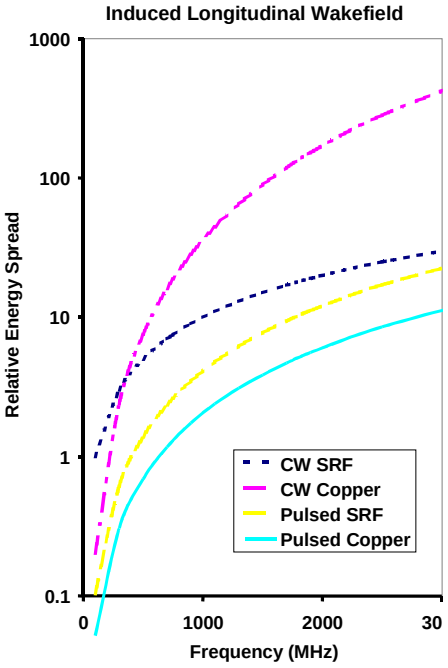

Figure 4: Longitudinal heating limits as a function of frequency. The scaling has assumed a fixed total linac energy, R/Q for each system based on the values quoted above, and micropulse length and cavity geometry ~ 1/f.

The transverse wakefield scales like [5]

$$dE \sim (Q/a^3)(g\sigma)^{1/2} L_{acc} / [\, l_{cell} \sqrt{N_{cell}}] \qquad (7)$$

up to Neff = ka^2/l_{cell}

L_{acc} is the linac length, and l_{cell} is the cell length.

Figure 5 illustrates the results of this scaling versus frequency. Again there is no particular advantage to srf operating pulsed. In CW operation the copper cavities can never overcome the severe handicap given by the small apertures in the system.

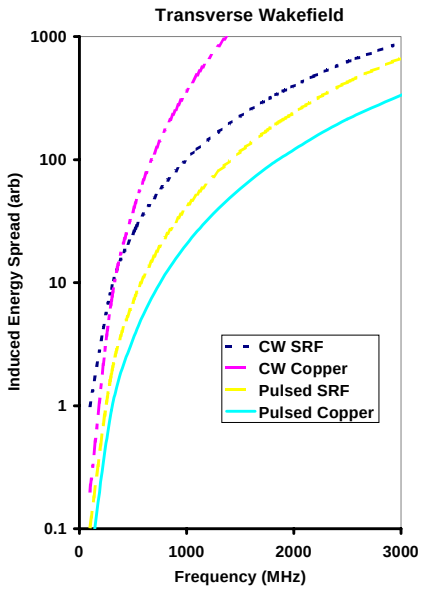

Figure 5: Transverse heating limits as a function of frequency.

The last physics parameter we consider is BBU. The specific threshold for regenerative BBU to occur is lattice dependent but that decision is essentially independent of copper versus srf technology and so is ignored We also ignore pulsed systems since regenerative BBU has little time to grow in a pulsed system. Moreover recirculating a pulsed beam generally offers little advantage. The threshold for BBU is [5]

$$I_{th} \sim 1/[\omega^2 \times L_{acc} \times Q_{HOM}] \qquad (8)$$

up to Neff, as in Equation 7.

Here the benefit in length and Q_{HOM} by 3x each again gives nearly an order of magnitude benefit to srf operating CW as shown in Figure 6. It is also clear from Figures 4 - 6 that if CW operation is desired then there is a significant push toward lower frequencies if stable operation is essential. At the lowest frequencies copper cavities become competitive in terms of physics performance although the cost penalties paid for the rf wall losses in CW operation are large.

2.2 System Implications

It is apparent from the above discussion that for an equivalent design, the srf machine offers the potential of a cleaner beam or equivalently can transport a larger current. This capability may be put to effective use in the

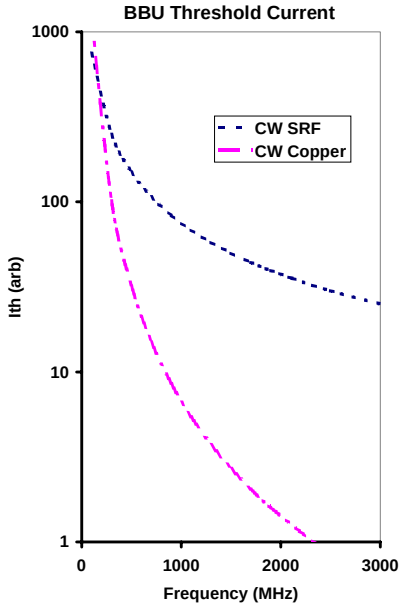

Figure 6: BBU limits as a function of frequency.

machine layout by recirculating the beam to higher energies in one linac (the approach that CEBAF uses toget 5 GeV beam from 800 MeV of linac) or operating the second pass 180 degrees out of phase to decelerate the beam and convert its power back to RF energy. Such a technique was used with FEL lasing in a copper accelerator but utilizing a second accelerator to decelerate the beam and couplers to feed the energy back to the first structure[8]. Instabilities were observed under some operating conditions. The technique of same cell energy recovery has also been demonstrated without lasing [9] and more recently while lasing[10]. The implications of such an approach are best illustrated by example. In what follows we present measurements from the Jefferson Lab IR Demo.

2.3 Implications of using same cell energy recovery

The motivation to use energy recovery as a key feature in the IR Demo design was to demonstrate the efficient and cost effective scalability of the system to yet higher average powers [11]. Because of the low electron beam energy (48 MeV) it does not yet substantially improve the

wall plug efficiency (only 2x to 3x). The tables below show measured and projected AC power consumption on the system. It should be emphasized that the following systems have not been optimised for low power consumption.

In the absence of energy recovery the AC power for linac RF would have been increased by 500 to 900 kW at the same efficiency achieved in the injector RF supply. Energy recovery has thus improved system performance by 58% to 64%. The benefits will be even more striking at higher beam energies and powers shown in Table 2. For a scale-up to 10 mA, 160 MeV, energy recovery will improve system performance by roughly 78%, reducing power draw from ~ 4700 kW to ~1075 kW. The required RF generation will be reduced by over 1700 kW saving on the order of $ 5M in capital costs. These factors becomes even stronger as the power of the FEL grows to the very high levels required for an industrially useful device (~ 100 kW) resulting in > 6% wallplug efficiency.

Table 1: IR Demo AC Wall Plug Powers

	With ER	Without ER
Injector RF	220 kW	220 kW
Linac RF	175 kW	700 kW
He refrigerator	70 kW (est.)	70 kW (est)
Magnets, Computers, etc.	43 kW	23 kW
Total	**508 kW**	**1013 kW**

Table 2: IR Upgrade and 100 kW Industrial Prototype AC Wall Plug Powers

	Upgrade With ER	Upgrade Without ER	Prototype With ER
Injector RF	350 kW	350 kW	750 kW
Linac RF	525 kW	4200 kW	650 kW
He refrigerator	100 kW (est.)	100 kW (est.)	100 kW
Magnets, Computers, etc.	100 kW	40 kW	100 kW
Total	**1075 kW**	**4690 kW**	**1600 kW**

The use of energy recovery brings additional benefits to the IR Demo beyond reducing the rf capital cost and improving the system electrical efficiency:

1) it reduces the dissipated power in the beam dumps by > 4x. The electron beam is transported with virtually no losses to the dump so the power that must be handled on the dump face is reduced by the energy ratio (10 MeV/48 MeV = 0.21) times to 50 kW from 240 kW. In a higher power accelerator, say 10mA at 160 MeV, this advantage is even more striking: to 100 kW from 1600 kW.

2) it virtually eliminates induced radioactivity in the dump region by dropping the terminal energy below the photo-neutron production threshold. For a copper beam dump reducing the energy to below 10 MeV can essentially eliminate the neutron production which activates surrounding components. Operating experience on the IR Demo has radiation backgrounds during running reduced by 10^4 or more increasing lifetimes of electronic components and significantly impacting the ease with which system maintenance can be performed.

However, there were several technical issues that had to be addressed to take advantage of such an energy recovery approach**:** stability of the electron beam, stability of the lasing process in such an energy recovered system, management of transport of large energy spread beams with low beam loss, and minimization of coherent synchrotron radiation induced emittance growth. These were all successfully handled by design optimizations as discussed in the references [12,13,14]. The cost of the recirculation arcs, while significant, are less than rf savings.

2.4 Implications of CW operation

Operation in a continuous wave mode is natural for srf systems. The low wall losses and large Qs mean the small penalties in providing refrigeration for operating a machine CW are offset by the relative ease with which CW rf can be generated and controlled with feedback. In comparison to typical copper machines which operate at 10^{-3} duty factor, operating CW can provide sizeable increases in FEL output power without invoking new laser physics. This is best illustrated by Figure 7 which shows the operation barrier reached by FELs before invoking CW operation in srf machines. Such a

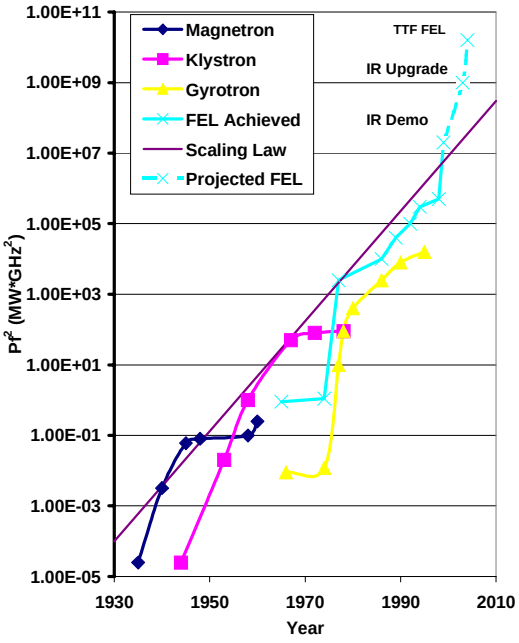

Figure 7: A time history of progress in electron operated radiation devices. Projected performance of the IR Upgrade and the TTF FEL is also shown. Adapted from [15].

breakthrough in technical approach is expected to produce not only further advances above the line of typical development but in the reasonably near future a 4th generation X-ray User facility providing light to many end stations at fluences 5 orders of magnitude or more higher than available today. The scientific possibilities are enormous.

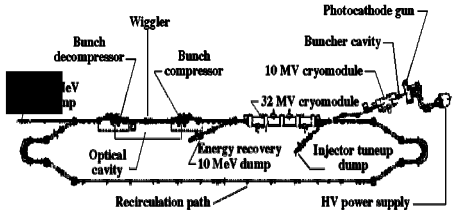

Figure 8: The IR Demo FEL

3 WORLD SRF FEL FACILITIES

Table 3 lists the operational and planned srf FEL facilities around the world. Progress in this area has been steady and encouraging. There are now 5 operational srf facilities around the world and of those 2 are User facilities where outside researchers can perform photonics research using the FEL. To gain insight into the panorama of possibilities we discuss below two examples: a state of the art facility in the infrared, the Jefferson Lab IR Demo in Virginia, and a facility to be brought into operation in the near future, the TTF FEL facility at DESY in Germany.

Table 3. World SRF FEL Facilties
Those in italics are under construction or commissioning. See [REF] for references on each system.

Country	Institution	Device	λ(μm)	τ_p(ps)	E_b/I_b (MeV/A)	P_{peak} (MW)	P_{avg} (W)	Accelerator freq. (MHz)
USA	SU	FIREFLY	19-65	1-5	20/14	.3	.4	1300 Pulsed (CW)
		SCA/FEL	3-10	0.7	37/10	10	1.2	1300 Pulsed (CW)
	JLab	IR Demo	3-8	1-2	48/60	25	1700	1497 CW
		IR Upgrade	*.2-25*	*0.5-2*	*160/100*	*150*	*10000*	
Germany	*Rossendorf*	*ELBE*	*5-150*	*1-2*	*40/50*			*1300 CW*
	DESY	*TTF FEL*	*0.04-0.2*	*.8*	*390/500*	*2000*	*7200*	*1300 Pulsed*
	Darmstadt	S-DLINAC	3-10	2	50/2.7	.15	3	3000 CW
Japan	JAERI	SCARLET	24-28	10	20/10	1	0.2	500 Pulsed (CW)

3.1 Example 1: The Jefferson Lab IR Demo FEL

The IR Demo installation was completed in September 1998. The layout is shown in Figure 8. The injector is the critical technology for operation of systems such as this; it must produce high average currents at high brightness. Although ultimately a srf photocathode gun such as under development in Dresden [17] is believed to be the most desirable, this system utilizes a DC photocathode operating at 320 kV to produce a 37.4 MHz pulse train of 60 pC [18]. The 20 ps beam is bunched by a copper fundamental cavity to around 3 ps and accelerated to 9.5 MeV in a srf cavity pair operting at 1497 MHZ. The beam is then accelerated to 36 to 48 MeV in a slightly modified CEBAF cryomodule. The beam is bent around the optical cavity mirror in a chicane, compressed by the chicane dispersion working on a slight energy slew of the micropulse and sent through the wiggler with roughly 60°A peak current in a micropulse of less than 1 ps FWHM. Approximately 0.5% of the electron beam energy is extracted in the NdBFe hybrid wiggler with 40 periods of 2.7 cm. The waste beam now has a large energy spread; full width can exceed 6%. Nonetheless, the beam is brought around the second mirror in an identical chicane, then through a 180 degree arc based on the Bates design [19]. A FODO lattice brings the beam to another arc and the beam is re-injected to the accelerator in the deceleration phase of the rf. As the beam decelerates its energy spread is compressed and the resultant beam is dumped at 10 MeV, now with less than 6% full energy spread.

When operated without energy recovery the beam current is limited by rf power to 1.1 mA average producing over 300 W from the FEL. In recirculation mode the recovered beam energy permits operation to the gun HVPS average current limit of 5 mA. Figure 9 shows the measured rf power in several cavities illustrating the

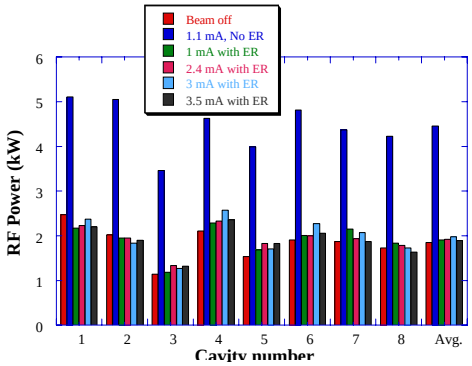

Figure 9: Measured rf power with and without energy recovery.

independence of rf power on accelerated current. Nearly 250 kW of electron beam power is being generated from 66 kW of rf without the limitations of electron cooling time or instabilities that would occur in a storage ring system.

When optimized the laser has produced up to 1.7 kW at 3 microns in this mode. This is 150 times the power of any other FEL in the world. The wavelength produced by the FEL is controlled by the electron beam energy. Suitable mirrors must be used for each wavelength band. To date the system has lased in three wavelength bands as shown in Figure 10. In addition, the system has produced watts of power lasing on the fifth harmonic at 1 micron [20].

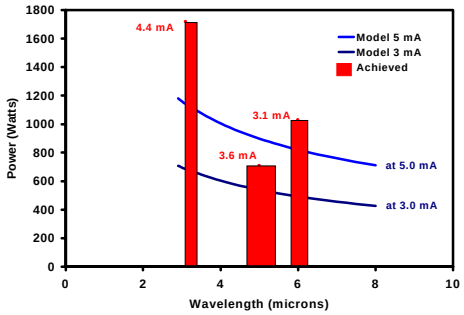

Figure 10: Projected and Achieved performance of the IR Demo FEL.

Building on the successful performance of the IR Demo an upgrade to the system is planned to establish shorter wavelength lasing at 1 micron and less and increase the power to 10 kW and beyond (see Figure 11). The system will be similar in layout but utilize 3 cryomodules including a new upgraded cryomodule with 40% more active length and high gradient capability. Additions of a short wavelength optimized wiggler and second optical cavity will permit high average power operation in the UV.

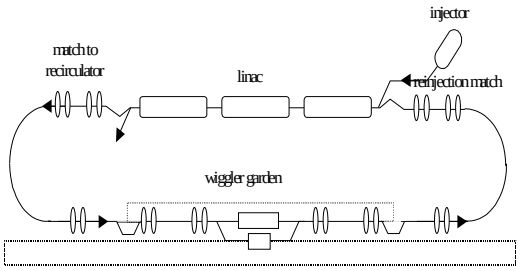

Figure 11: Schematic layout of the IR/UV Upgrade FEL.

Additional FELs will soon offer the benefits of CW operation. An upgrade of the Stanford SCA us underway using TESLA cavities and a new refrigerator which will permit CW operation. Already one of the most productive FEL user facilities in the world, this capability with further enhance its operation for scientific research. Plans are also underway for an upgrade of the JAERI FEL to high duty factor and the construction of a machine similar to the upgraded SCA in Dresden.

3.2 Example 2: The TTF FEL

Going to yet shorter wavelengths will be the TTF FEL now in commissioning at DESY [21]. It is designed as a proof of principle device for a planned 4th Generation Light Source Facility. While srf technology is not required to reach the short wavelengths, its use is essential for a 4th Generation User facility in order to achieve the duty factor required to service many users. The concept is to switch the beam among a farm of wigglers with a user experiment at the output of each.

The brightness produced from this device in subpicosecond pulses goes orders of magnitude beyond what is currently available and is expected to open up new fields of research. Initial capability of the machine is 40 nm; beam is already being produced in the linac and demonstrations of amplification are to follow soon. The desired wavelength is so short that efficient mirrors do not exist so the machine operates in a Self-Amplified Spontaneous Emission (SASE) mode where sufficient gain per pass exists to saturate the FEL in a single pass through the wiggler. Such systems require extremely high peak beam currents, and exceptional beam quality. The TTF FEL plan is to eventually reach a wavelength of 6.5 nm using a 1 GeV 2500A electron beam pulse. The wiggler would be 27 m to saturation and have a peak field of 5 kG and a period of 2.73 cm. The peak power is anticipated to reach 2 to 3 GW. Later an energy upgrade to 50 GeV will result in photon energies up to 10 keV and average brilliances of 10^{26} photons/sec/mm^2/0.1% BW. This extraordinary light source will offer unprecedented opportunities for research into the fundamentals of photon/matter interactions.

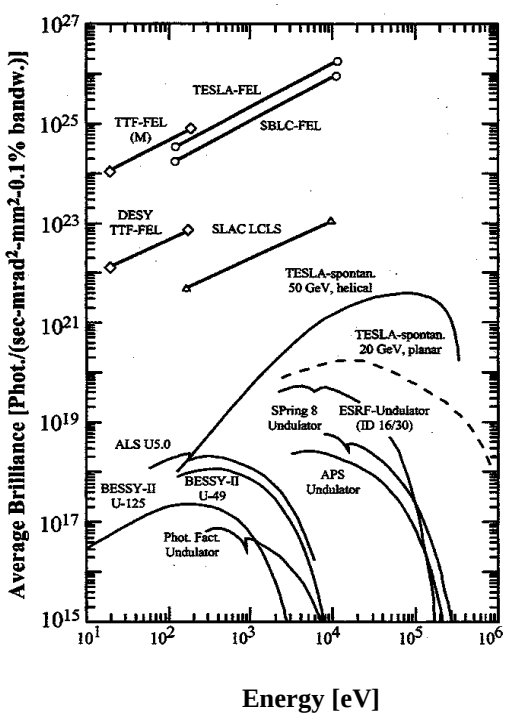

Figure 12: Performance of the TTF FEL device. Figure courtesy of J. Rossbach.

4 SUMMARY

SRF technology has provided a capability for high duty factor operation of FELs that has wide ranging implications. It offers improved beam quality. It permits the use of system designs incorporating same cell energy recovery for high efficiency at high power. Its use has already permitted operation of an FEL at average power levels 150 times competing copper systems. In the future it will be incorporated into a high power SASE UV demonstration system and ultimately User facility. This User facility will take advantage of the high duty factor operation to multiplex the FEL beam among many groups making practical the 4th Generation Light Source through cost sharing between many groups. It is further expected that future improvements in SRF technology will make its system advantages of high duty factor operation and excellent beam quality provided even more compelling.

5 ACKNOWLEDGEMENT

I depended on discussions with many members of the Jefferson Lab staff in the development of this paper. I would like to especially acknowledge the contribution of Lia Merminga to perform the analysis of beam stability and the help of Peter Kneisel in reviewing the status of srf development. Errors in interpretation are my own. The break-though performance of the IR Demo FEL was the result of a team effort which I depended on and am happy to acknowledge. This work was supported by U.S. DOE Contract No. DE-AC05-84-ER40150, the Office of Naval Research, the Commonwealth of Virginia and the Laser Processing Consortium.

6 REFERENCES

[1] S. Benson, private communication. See also G. Dattoi, et al. “Intensity Saturation Mechanism in Free Electron Lasers”, IEEE J. Quant. Elect. QE-28 (1992) pgs 770-772. The overlap dependence has been added and the degradation factors normalized to one compared to the formula from this reference.

[2] M. Xie, “Design Optimization for an X-ray Free Electron laser Driven by SLAC Linac” Proceedings of the 1995 Particle Accelerator Conference (Dallas, 1995) pgs. 183-186.

[3] C. L. Bohn, "Recirculating Accelerator Driver for a High-Power FEL: A Design Overview", Proc. 1997 Part. Accel. Conf., IEEE Cat. No. 97CH36167, (1998) pgs 909-911.

[4] J. Kirchgessner, “Review of the Development of RF Cavities for High Currents”, Proceedings from the 6th Workshop on RF Superconductivity, Newport News, VA, (1993) pgs 331-336.

[5] L. Merminga, "BBU Scaling Laws" to be published as CEBAF Tech Note.

[6] Thomas Wangler, RF Linear Accelerators, John Wiley & Sons, (1998) pg 160.

[7] Hasan Padamsee, Jens Knobloch, Tom Hays, RF Superconductivity for Accelerators, John Wiley & Sons, (1998) pg 284.

[8] Donald Feldman, et al., Nucl. Instr. and Meth. in Phys. Rsch. A259 (1987) pgs 26-30.

[9] T. I. Smith, Nucl. Instr. and Meth. in Phys. Rsch. A259 (1987) pgs 1-7.

[10] George R. Neil, et al., “High Average Power Lasing in an FEL with Same Cell Energy Recovery”, Proceedings of FEL’99, to be published in Nucl. Instr. And Meth. in Phys. Rsch. (2000).

[11] S. Benson, et al, “First Lasing of the Jefferson Lab IR Demo FEL”, Nuclear Instruments and Methods in Physics Research A 409 (1999) 27-32.

[12] Campisi, I., Douglas, D., Hovater, C., Krafft, G., Merminga, L., Yunn, B., "Beam Current Limitations in the Jefferson Lab FEL: Simulations and Analysis of Proposed Beam Break-up Experiments". Proceedings of the 18th Particle Accelerator Conference (PAC 99), New York, NY, March 29-April 2, 1999.

[13] Merminga, L., Alexeev, P., Benson, S., Bolshakov, A., Doolittle, L. and Neil, G., “Analysis of the FEL-RF Interaction in Recirculating, Energy-Recovering Linacs with an FEL” Nuclear Instruments and Methods in Physics Research A 429 (1999) 58-64.

[14] D. Douglas, “Lattice Design for a High-Power Infrared FEL”, Proceedings of the 1997 Particle Accelerator Conference, Vancouver, B.C., Canada, May 11-15, 1997.
[15] H. P. Freund and G. R. Neil “Free-Electron Lasers: Vacuum Electronic Generators of Coherent Radiation”, Proc. IEEE Vol. 87, No. 5, (May, 1999) pgs. 782-803.
[16] W. B. Colson, “Short Wavelength free electron lasers in 1998”, Nucl. Instr. and Meth. in Phys. Rsch. A429 (1999) 37-40.
[17] D. Jansen, et al., Proc. of the 1997 Particle Accelerator Conf., Vancouver, Canada (1997).
[18] D. Engwall, C. Bohn, L. Cardman, B. Dunham, D. Kehne, R. Legg, H. Liu, G. Neil, M. Shinn, C. Sinclair, "A High-DC-Voltage GaAs Photoemission Gun: Transverse Emittance and Momentum Spread Measurements", Proc. 1997 Part. Accel. Conf., (1998) pgs. 2693-2695.
[19] J. B. Flanz and C. P. Sargent, "Operation of an Isochronous Beam Recirculation System," Nucl. Inst. And Meth in Phys Research. A241 (1985) pgs 325-333.
[20] S. Benson, et al., “5th Harmonic Lasing of a FEL", Proceedings of FEL’99, to be published in Nucl. Instr. And Meth. in Phys. Rsch. (2000).
[21] A VUV free electron laser at the TESLA test facility; conceptual design report, DESY Print TESLA-FEL 95-03, Hamburg, Germany, 1995.